AN ABSTRACT OF THE THESIS OF

Jesse A. Weller for the degree of Bachelor of Science in Physics presented on May 27, 2019.

Title: Beyond Scattering: Identifying the Boundaries of Light Control with a Genetic Wavefront Optimization Algorithm

Abstract approved: _____

Guenter Schneider

The ability to focus light through strongly scattering materials is opening up exciting new avenues in many fields, such as optics, computer vision, biology, and medicine, which utilize light delivery and imaging techniques. Efficient, high resolution wavefront shaping and optimization methods are crucial to enabling this new capability. In this thesis, we explore the limitations on focusing light through scattering media using a genetic optimization algorithm (GA), extending the work that has previously been done demonstrating light control through opaque materials. We test the performance of GA to focus a laser wavefront through a wide range of scattering materials using a phase-only spatial light modulator (SLM). In this work, we show that the composition of the scattering material significantly affects the ability to focus light. Previous work has demonstrated the dependence of the focus enhancement on the resolution of wavefront modulation. We confirm this conclusion and go further to show that the aspect ratio of the SLM segments (or partitions) also plays a determining role. Finally, we document significant limitations of using the signal-to-background ratio and the enhancement, η, as performance metrics in an experimental setting.

Beyond Scattering: Identifying the Boundaries of Light Control with a Genetic Wavefront Optimization Algorithm

by

Jesse A. Weller

A THESIS

submitted to

Oregon State University

in partial fulfillment of
the requirements for the
degree of

Bachelor of Science

Presented May 27, 2019
Commencement June 2019

Bachelor of Science thesis of Jesse A. Weller presented on May 27, 2019.

APPROVED:

Research Advisor, representing Physics

Director of the School of Physics

I understand that my thesis will become part of the permanent collection of Oregon State University libraries. My signature below authorizes release of my thesis to any reader upon request.

Jesse A. Weller, Author

TABLE OF CONTENTS

LIST OF FIGURES

Chapter 1: Introduction

1.1 Objective

The ability to efficiently focus light through a scattering medium has many applications in optics, computer vision, biology, and medicine. In the field of medicine, this ability could enable the delivery of light within tissues, opening up exciting new avenues in diagnostics, procedures, and drug delivery. In optics, the use of neural networks has turned scattering surfaces into lenses [1], and in computer vision this method has lead to breakthroughs in the identification of objects located behind opaque surfaces, such as a sheet of paper [2].

For most of history, scattering was seen as an obstacle to the effective control of light. However, with the invention of high resolution light control tools such as digital micromirror devices and spatial light modulators (SLM), it has become possible to prepare wavefronts with phase or amplitude modulation with resolution at the micrometer scale.

In this work, we simulate the focusing of an electromagnetic wavefront passing through strongly scattering media and use a type of machine learning algorithm, called a genetic algorithm (GA), to optimize the simulated wavefront. We then test the GA on a physical system in which an SLM is used to modulate a laser wavefront passing through a scattering sample. We use this experimental setup to test the limits to scattering control due to segment size, shape, and scattering sample material.

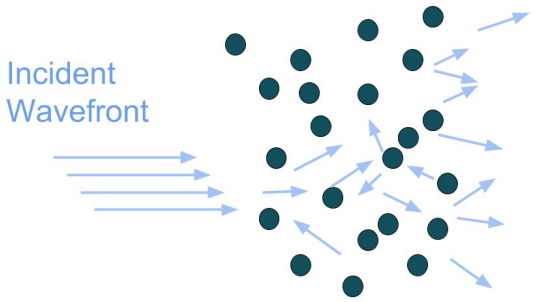

Figure 1.1: Multiple scattering. The figure depicts the multiple scattering of an incident wavefront by a strongly scattering medium.

1.2 Background

In strongly scattering materials the light from an incident wavefront is completely scrambled (Figure 1.1), creating a random speckle field in the output plane. However, it was recently discovered that the focusing of light through scattering media can be achieved through the optimization of a wavefront shaped by an SLM [3–7]. Using this method, the scattering effect of a medium can be overcome by preparing a plane wave in such a state that the transmission of the wave through the medium produces a desired speckle pattern or bright focal point.

The optimization of the wavefront is achieved through the use of either sequential or feedback based algorithms, controlling the pixel-wise phase or amplitude modulation. The general model is to partition the wavefront into equal sized areas, called "segments", and use an SLM to modulate the relative phase or amplitude of each segment. Segmentation is achieved by grouping the pixels of the SLM into larger blocks, so as to decrease the computational complexity of the algorithm, while maintaining a high degree of light control. Each set of modulations to the wavefront is referred to

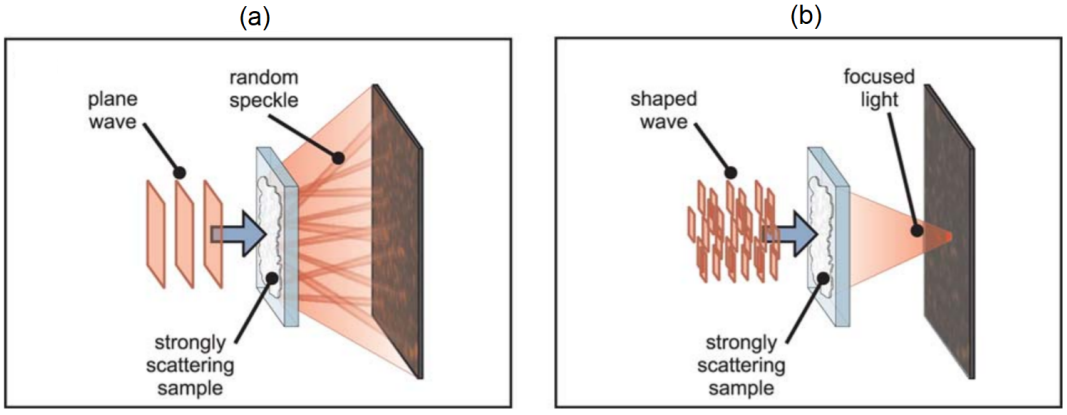

Figure 1.2: Wavefronts through scattering media. (a) Uniform wavefront produces a random speckle pattern in the output field. (b) Prepared wavefront produces focused point in the output field. Figure reproduced from [5].

as a mask. For example, a uniform mask would be one in which all of the segments, and therefore all of the pixels, have the same phase and amplitude value. In this work, we use a model based on phase-only modulation.

The optimization algorithm that we develop and test is in a class of so-called genetic algorithms (see section 2.2). These algorithms derive their inspiration from the field of evolutionary biology. The structure of the algorithm attempts to mimic the optimization process used in natural selection, which has proven to be very robust in noisy environments and applicable to a wide range of problems [7]. We analyze the performance of the GA as a wavefront optimizer in both simulated and experimental regimes.

Chapter 2: Materials and Methods

All coding was done in Python. Simulation of the scattering media and the transmission of the plane wave was implemented using a transmission matrix model:

$$E_m = \sum^{N} t_{mn} A_n e^{i\phi_n}, \tag{2.1}$$

where E_m is the complex field at the output segment m, A_n and ϕ_n are the amplitude and phase of the light from incident segment n. The segments of the input field (see Figure 2.1) are independently defined from the segments of the output field. Each are arbitrarily partitioned regions of the respective light field used for efficient computation (input field) or for defining a desired focal pattern (output field). The scattering process is represented by an $M \times N$ transmission matrix with elements t_{mn} which describe the linear relationship between the input and output segments.

2.1 Metrics

We analyze the performance of the optimization method under various conditions by using the enhancement η as a metric for the improvement of the target focus intensity I_β. The intensity of a general segment m is defined as:

$$I_m = \frac{1}{N}\left| \sum^{N} t_{mn} e^{i\phi_n} \right|^2 \tag{2.2}$$

Using the intensity of the focus, the relative enhancement of the output field focus is defined as

$$\eta = \frac{I_\beta}{< I_\beta >}, \tag{2.3}$$

where I_β is the intensity of the output field focus and $< I_\beta >$ is the intensity of the focus averaged over all possible ensembles of the transmission matrix for a given optimized mask. In a disordered scattering medium, since the constants t_{mn} of the transmission matrix (Equation 2.1) are statistically independent and follow a circular gaussian distribution, the maximum achievable enhancement for phase only modulation can be defined as

$$\eta_{max} = \frac{\pi}{4}(N-1) + 1, \tag{2.4}$$

where N is the number of modulation segments [5, 8]. In this work, we approximate $< I_\beta >$ by measuring initial average intensity of the output field before optimization, I_0 [6,7,9]. In each of our trials, we found I_0 by taking an average of the intensity of the output field created by 3000 random masks loaded onto the SLM. Another metric commonly used for similar applications is the signal to background ratio (SBR) which is defined as

$$SBR = \frac{I_\beta}{\sum\limits_{m \neq \beta} I_m}, \tag{2.5}$$

which is the intensity of the output focus divided by the background intensity after optimization. As is shown in our results (Section 3.2.3), the SBR is not a very reliable metric due to the coupled enhancement of the background intensity, especially when N is large. For this reason, the enhancement is usually the preferred metric.

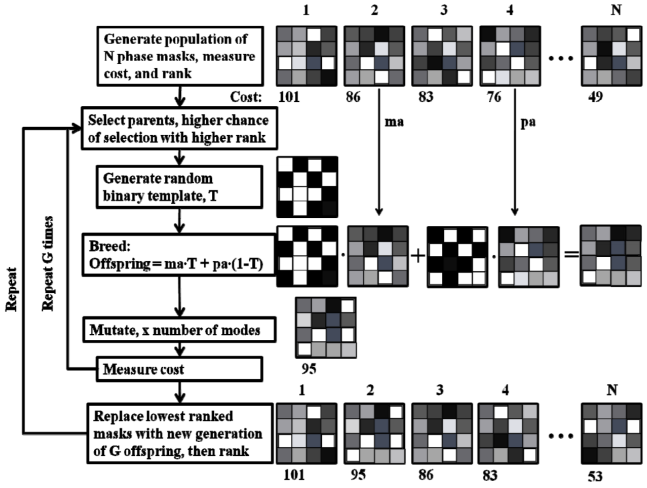

Figure 2.1: Block diagram showing steps of the genetic algorithm. Each phase mask in this diagram has 16 segments, or partitioned regions of the input field. The phase value of each segment can be independently controlled by the SLM. Reproduced from [7].

2.2 Genetic Algorithm

Optimization of the input field is achieved with a genetic algorithm. To begin, the algorithm generates an initial population of S input field masks, each with randomly chosen phase values. A cost function using intensity I_β at segment(s) β in output field is used to rank each of the S input field masks.

Two parent masks, P_1 and P_2 are then selected for breeding, with a higher probability of selection given to higher ranked masks. A new child mask is produced from the two parents by randomly generating a binary matrix T. The input segments of the two parents are combined to generate the new mask according to $Child = P_1 \cdot T + P_2 \cdot (1 - T)$. A random subset of segments of the child mask is then changed (mutated) to a random phase value. The mutation rate R is defined by

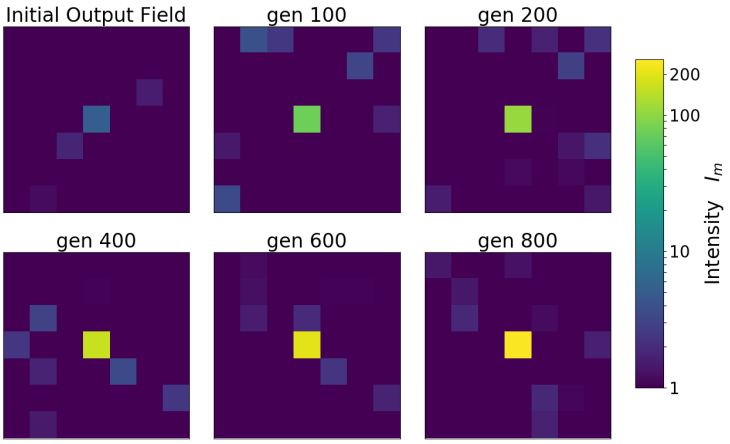

Figure 2.2: Output field (around focus) at various generations of the optimization process of the GA. The center pixel is used to calculate the intensity enhancement, I_m, which is maximized by the algorithm during each generation.

$$R = (R_0 - R_f) \cdot e^{\frac{-g}{\lambda}} + R_f, \tag{2.6}$$

where R_0 and R_f are the initial and final mutation rates, g is the generation number, and λ is the decay factor. The size of the mutated subset is determined by multiplying the mutation rate R by the total number of segments N. For each generation, a number of new masks, typically N/2, are created in this manner and the cost function is used to add each new mask to the population, replacing the lowest ranked mask. The algorithm is run for G generations, and for each generation the population of input masks effectively searches the solution space and maximizes the value of the cost function. In our case the result of the optimization process yields a bright speckle at a single output segment β (Figure 2.1).

2.3 Experiment

After testing it on the simulated model, the GA was applied to the experimental setup shown in Figure 2.3 in which a phase-only liquid crystal SLM was used to control light produced by an HeNe laser that passed through a scattering sample. An 8-bit CCD camera was used to record the intensity of the output field. We tested the performance of the GA over varying segment numbers, segment shapes, and scattering materials, using the enhancement η (section 2.1) as the primary metric for assessing the improvement in the output focus for each trial.

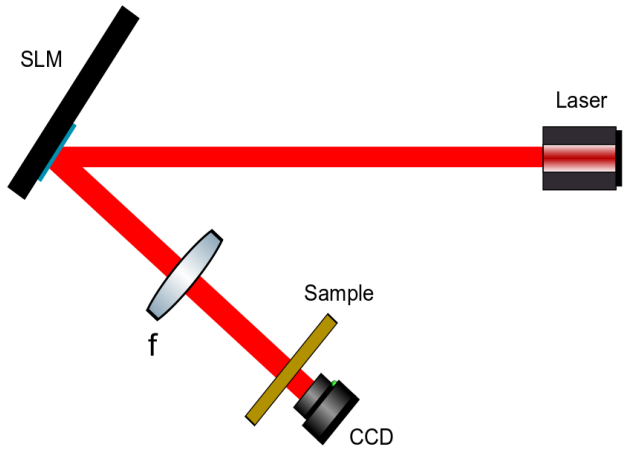

Figure 2.3: Experimental Setup: HeNe laser, phase-only Liquid Crystal Spatial Light Modulator (Cambridge Correlators SDE1024), focusing lens, scattering sample, and an 8-bit CCD camera (Imaging Source DMK21AU04). Lens placed halfway between SLM and Camera, one focal length f from each.

Chapter 3: Results and Discussion

3.1 Simulation

We tested the GA with the simulated model for varying number of segments, N. The results (Figure 3.1) show that the enhancement is proportional to the number of segments (see Equation 2.4) and inversely proportional to the segment size.

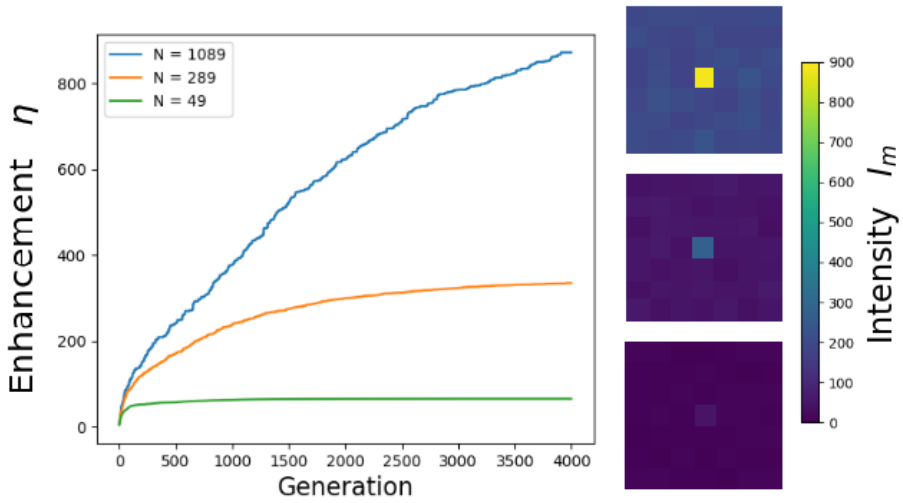

Figure 3.1: Left: Enhancement η (section 2.1) of output focus for each step (generation) of optimization process for varying number of segments, N. Right: Output intensity field after optimization process for varying number of segments, N.

3.2 Experimental

After testing the GA on the simulated system, we applied it to a physical system using various scattering samples (Fig. 3.2. The output fields before and after optimization are shown in Figure 3.3 using a thin piece of plastic as the scattering sample.

ID	Material	Description
bb1	plastic	Plastic with tiny air bubbles (bubble wrap).
gg1	glass	Ground glass plate.
PL1	plastic	Thin piece of projector plastic.
ps2	painted glass	Glass slide with grey matte paint.
ps4	painted glass	Glass slide with white glossy paint.
s1000	glass	Glass slide ground with 1000-grit sandpaper.
s220	glass	Glass slide ground with 220-grit sandpaper.
s120	glass	Glass slide ground with 120-grit sandpaper.
sclear	glass	Glass slide (clear).
vellum	paper	Single layer of white vellum paper.

Figure 3.2: Table of scattering samples used in this paper.

In Figure 3.4, experimental data is shown for the enhancement achieved when focusing light through a scattering sample for a varying number of segments, N. As with the simulated model, we found enhancement to be proportional to N (see Equation 2.4).

3.2.1 Segment Shape

In Figure 3.5, the enhancement is shown for a single sample while varying N and segment shape. The plot shows that, for this sample, a segment shape of 64x96 (N=128) achieved a higher enhancement than a segment shape of 96x24 (N=341). While the enhancement achieved is generally proportional to N (see Equation 2.4), the plot shows that segment shape (or aspect ratio) is also a significant

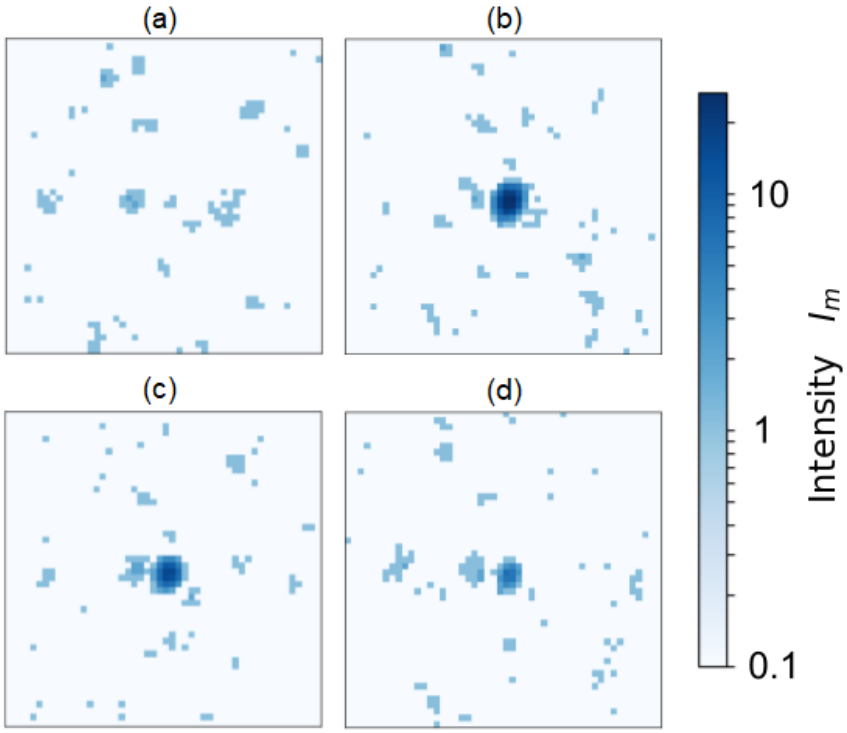

Figure 3.3: Speckle field and focused fields in optimization experiment. (a) Initial speckle field. Focused fields after optimization with (b) N=1024, (c) N=256 (d) N=64. The scattering sample was a thin piece of plastic.

factor. In our trials a lower aspect ratio performed better, but the ideal shape of segment may depend on the configuration of the optical system or the structure of the scattering material.

3.2.2 Scattering Material

We tested scattering control for various samples (see Table 3.2 for descriptions) using a fixed segment size and compared the enhancement achieved for each sample. In Figure 3.6 the results show a wide range of achieved enhancements. From the data, we can conclude that the properties

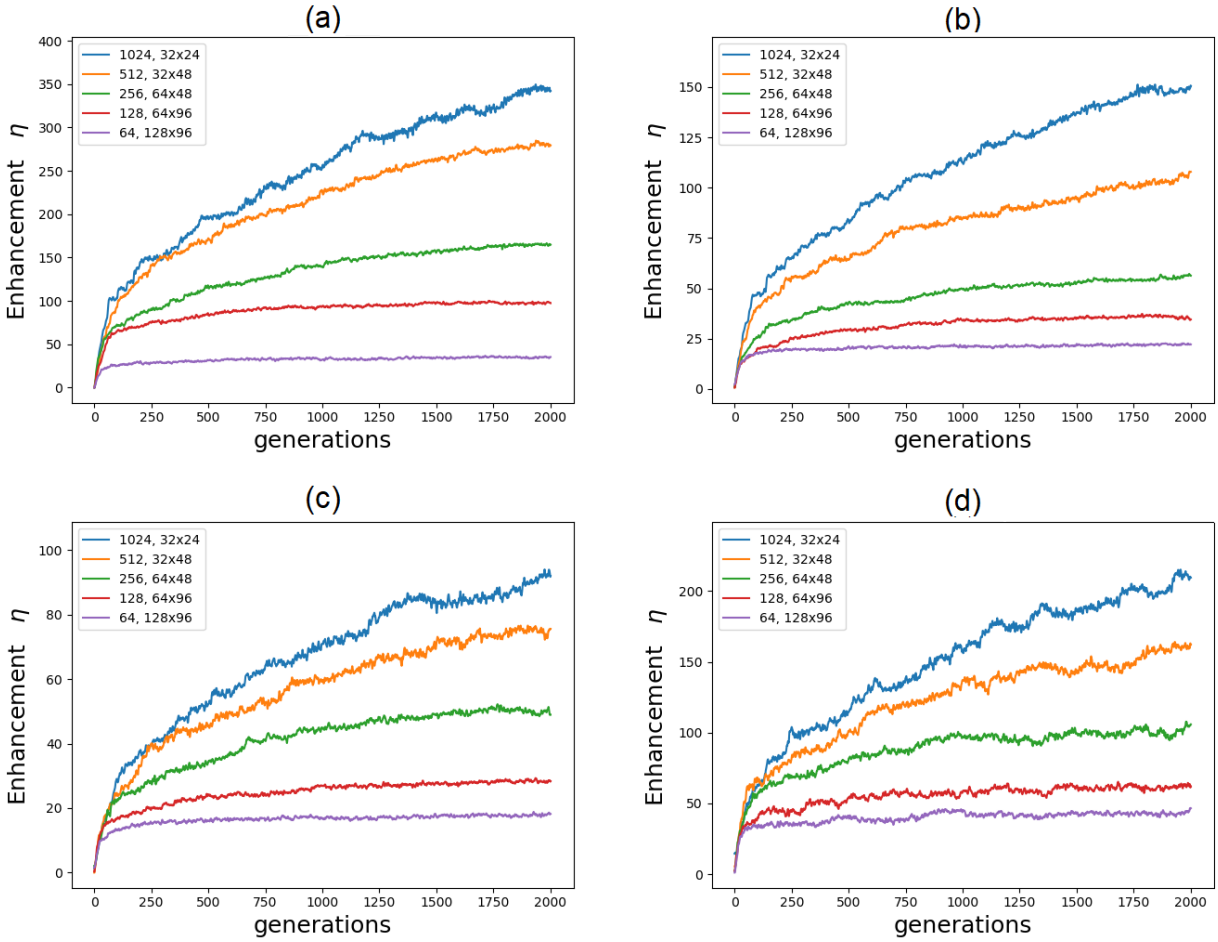

Figure 3.4: Enhancement plot for genetic algorithm optimization experiment for multiple samples and varying segment shape (*width* × *height*) and number of segments (shown in legend). Samples (Fig. 3.2) in figure are (a) bb1, (b) ps2, (c) PL1, (d) vellum.

of the scattering material are a significant factor in determining the limits to scattering control. A clear example of this dependence comes from looking at the performance of the two trials with painted slide samples *ps2* (matte paint) and *ps4*(glossy paint). Sample *ps2* ($I_0 = 0.12$) achieved almost double the enhancement of *ps4* ($I_0 = 0.04$), despite having a higher initial average intensity

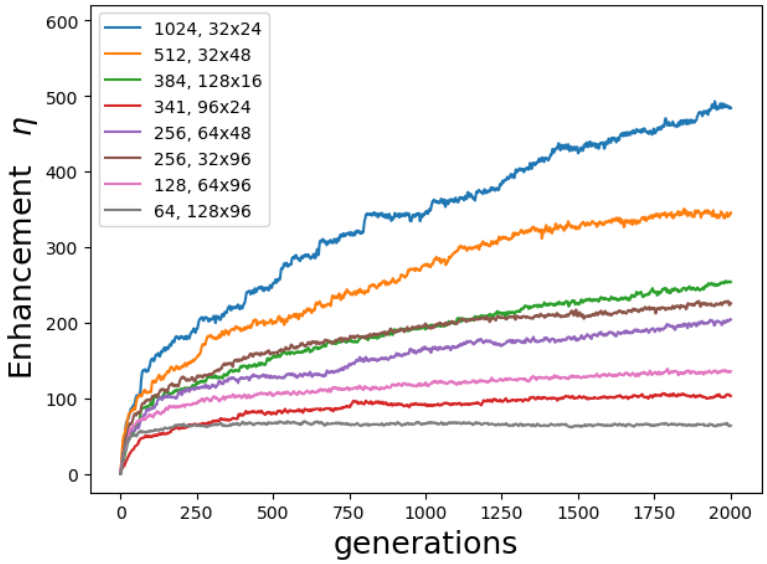

Figure 3.5: Experimental data for the enhancement of the output focus for each step (generation) of optimization process for varying number and shape (*width* × *height*) of segment (shown in legend). The scattering sample *gg1* (Fig. 3.2) was a piece of ground glass.

(see Section 3.2.3 for a description of η dependence on I_0). In this case the reflectivity of the paint is a possible explanation for the difference in focus enhancement achieved. The performance difference due to material properties can also be seen for samples *s1000, s220, s120, sclear, and gg1*, which are all glass materials. The only difference between them is the level of roughening of their surfaces. Despite this material similarity the enhancement achieved varies between them, though less drastically than it appears in Figure 3.6 due to I_0 bias (see Section 3.2.3).

3.2.3 Metrics

We tested the ability of two common metrics (see Section 2.1) to accurately describe the improvement in the intensity of the focus region after optimization: the enhancement η (equation 2.3) and

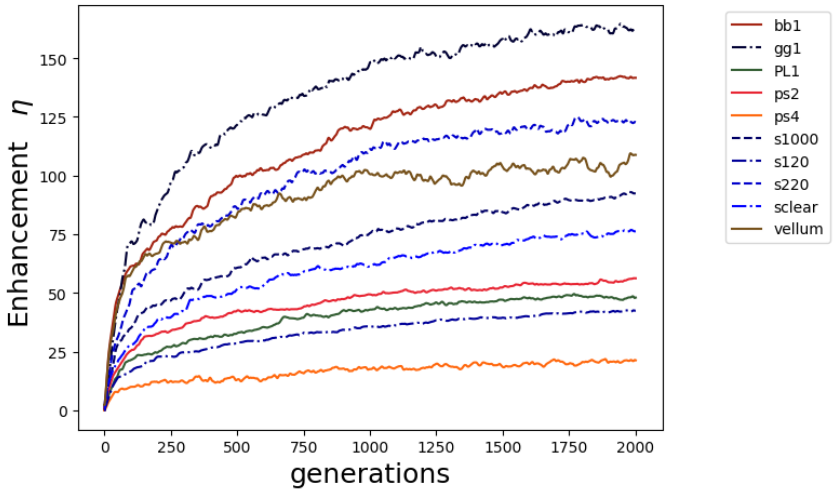

Figure 3.6: Experimental data for the enhancement of the output focus for each step (generation) of optimization process for various scattering samples (see Table 3.2 for descriptions) with N=512, segment size 64x48. The data in this figure is smoothed for ease of interpretation.

the signal to background ratio (equation 2.5). When we used a painted slide (ps2) as a scattering sample, the extreme difference in the two metrics is clearly seen (Figure 3.8). To help understand the discrepancy, we looked at the output fields and background intensity shown in Figure 3.7.

For this material, the background intensity increased along with the focus intensity, and the brightening of the background intensity is stronger in trials with a higher number of segments, N. This shows that the SBR metric is highly dependent on background intensity, so it is not a very robust performance metric for determining the improvement of the focus intensity. The enhancement does not show this particular bias, and is therefore a superior metric for this application.

However, the enhancement must also be used carefully due to its dependence on I_0, which is our approximation of $< I_\beta >$ (see Section 2.1). By comparing the trials with glass slide samples (Figure 3.9 it is obvious that the value of η is dependent on the value for the initial average intensity I_0. This can be clearly seen by looking at the trials using the same scattering sample, *gg1*. The

enhancement achieved has a significant sensitivity to the value of I_0.

Although this bias explains most of the variation in the achieved enhancement between the glass slide trials, there is still variation between the materials. For example, the trial for sample *sclear* ($I_0 = 0.13$) produced a slightly higher enhancement than the trial with sample *gg1* ($I_0 = 0.088$). Similarly for the two trials performed with painted slides (seen in Figure 3.6), the initial intensity for the trial with sample *ps2* (I_0=0.12) was much higher than for the trial with sample *ps4* (I_0=0.04), yet the achieved enhancement for *ps2* was double that of *ps4*. Therefore the dependence on sample material shown by our results in Section 3.2.2 still stands despite this bias.

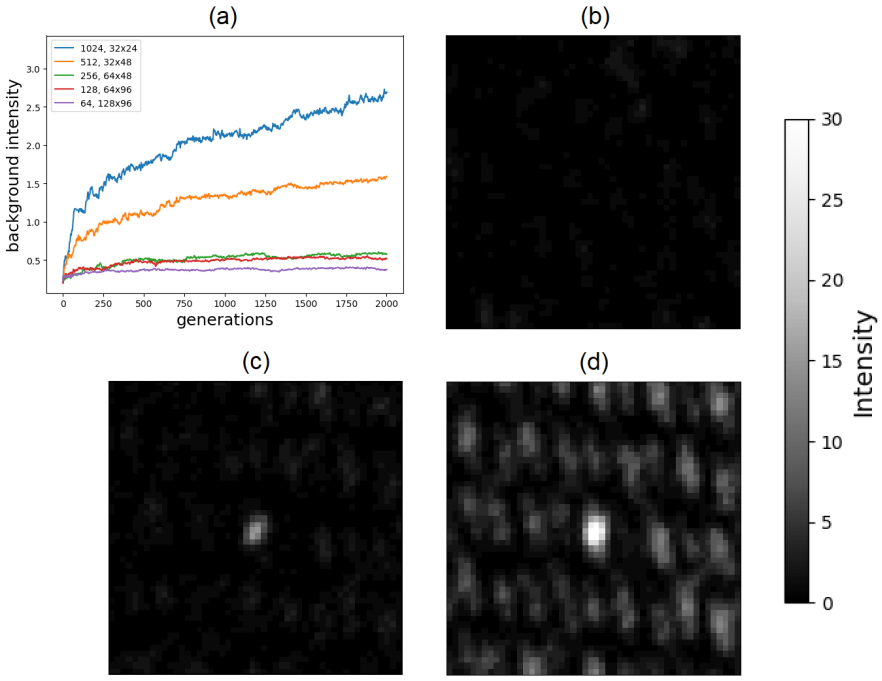

Figure 3.7: Background intensity and output fields for the optimization process using a painted glass slide sample (ps2). (a) Background intensity plot. The number and shape (*width* × *height*) of segments are shown in legend. (b) Initial speckle field before optimization. (c) Output field after optimization, N=1024. (d) Output field after optimization, N=256. Comparison of (c) and (d) shows an increase of the background intensity along with the focus intensity for higher N.

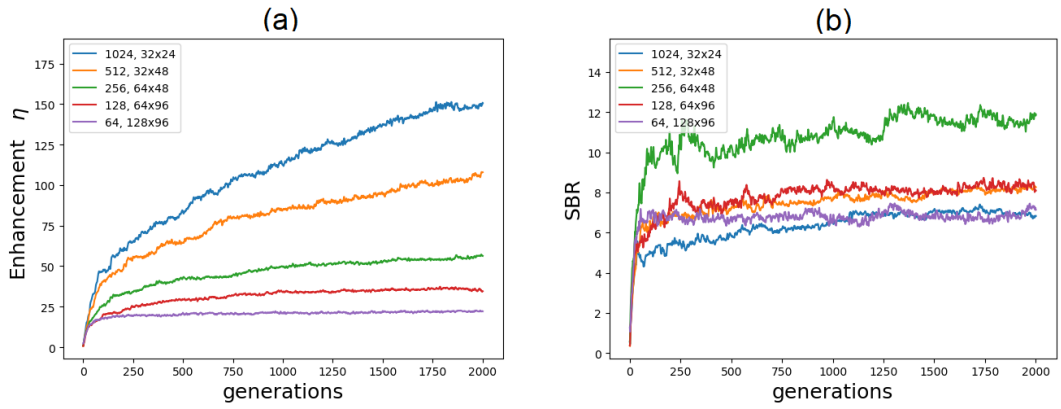

Figure 3.8: Comparison of the (a) enhancement and (b) SBR metrics for a scattering sample. Sample is a painted glass slide (ps2). The number and shape (*width* $\times$ *height*) of segments are shown in legends.

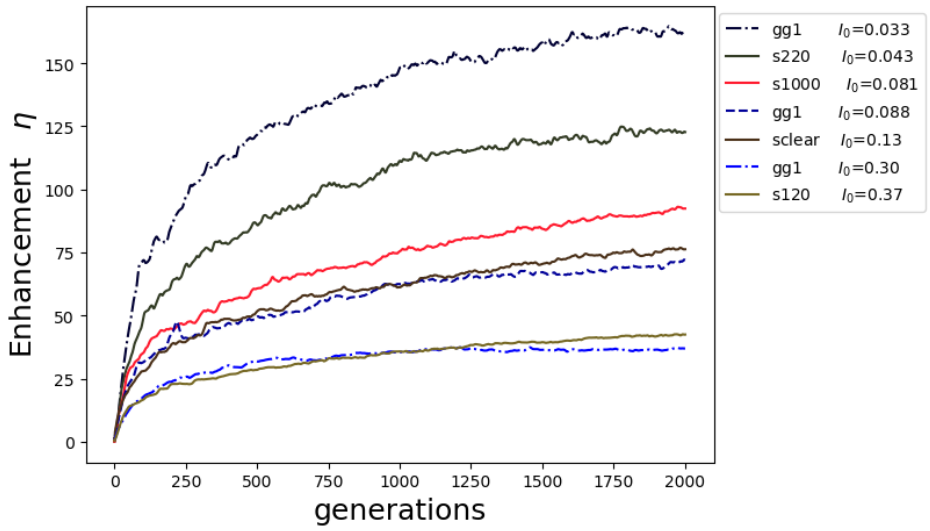

Figure 3.9: Comparison of the enhancement achieved for all trials using glass slides as samples. A clear dependence of the optimized enhancement metric on the initial average intensity I_0 is shown.

Chapter 4: Conclusion

The ability to focus light through strongly scattering materials is opening up new avenues in light delivery and imaging. Efficient, high resolution wavefront shaping and optimization techniques are crucial to enabling this new capability. Our goal in this paper was to identify and analyze some of the limitations to scattering control in a system using a GA to optimize an incident laser wavefront with a phase modulating SLM.

Our results found that the most significant limitation to scattering control is the composition of the scattering material. We confirmed the results of previous work [5–7] showing that the enhancement of the focus is proportional to the resolution of wavefront modulation, but we also found that the shape of the segments (or partitions) of the modulated wavefront also has a significant effect, with a lower aspect ratio generally performing better. Finally, we documented major limitations of using the signal-to-background ratio (due to target-background intensity coupling) and the enhancement η (due to initial average intensity measurement bias) as performance metrics in an experimental setting. We concluded that η remains the most robust metric if used with sensitivity toward this limitation.

Future work to extend this research could take a number of paths. Although we showed that scattering material composition generally affects the limitations of scattering control, it may be useful to characterize the limiting effect of specific material properties. Applications in imaging through static scattering media are already being explored, including some approaches using neural networks [1,2]. A similar study could be done in testing the limits of imaging, or classifying objects, through media of varying properties. To our knowledge, no such studies have yet been undertaken.

Bibliography

[1] A. Sinha, J. Lee, S. Li, and G. Barbastathis. "Lensless computational imaging through deep learning". Optica, **4**(9), 1117–1125, 2017.

[2] G. Satat, M. Tancik, O. Gupta, B. Heshmat, and R. Raskar. "Object classification through scattering media with deep learning on time resolved measurement". Opt. Express, **25**(15), 17466–17479, 2017.

[3] A. P. Mosk, A. Lagendijk, G. Lerosey, and M. Fink. "Controlling waves in space and time for imaging and focusing in complex media". Nature Photonics, **6**(5), 283–292, 2012.

[4] B. R. Anderson, P. Price, R. Gunawidjaja, and H. Eilers. "Microgenetic optimization algorithm for optimal wavefront shaping". Applied Optics, **54**(6), 1485–1491, 2015.

[5] I. M. Vellekoop and A. P. Mosk. "Focusing coherent light through opaque strongly scattering media". Optics Letters, **32**(16), 2309–2311, 2007.

[6] I. M. Vellekoop. "Feedback-based wavefront shaping". Optics Express, **23**(9), 12189–12206, 2015.

[7] D. B. Conkey, A. N. Brown, A. M. Caravaca-Aguirre, and R. Piestun. "Genetic algorithm optimization for focusing through turbid media in noisy environments". Optics Express, **20**(5), 4840–4849, 2012.

[8] J. W. Goodman. Statistical optics. Wiley, Hoboken, New Jersey, 2nd ed. edition, 2015.

[9] S. M. Popoff, G. Lerosey, R. Carminati, M. Fink, A. C. Boccara, and S. Gigan. "Measuring and exploiting the transmission matrix in optics". In "Conference on Lasers and Electro-Optics 2010 (2010), paper QME6," page QME6. Optical Society of America, 2010.